Geoderma 403 (2021) 115276

Contents lists available at ScienceDirect

Geoderma

journal homepage: www.elsevier.com/locate/geoderma

Biochar application driven change in soil internal forces improves aggregate stability: Based on a two-year field study

Feinan Hu [a,b,c], Chenyang Xu [a,b], Rentian Ma [a,b], Kun Tu [a,b], Jiayan Yang [a], Shiwei Zhao [a,b,c], Mingyi Yang [a,c], Fengbao Zhang [a,c,*]

[a] State Key Laboratory of Soil Erosion and Dryland Farming on the Loess Plateau, Northwest A&F University, Yangling 712100, China
[b] College of Natural Resources and Environment, Northwest A&F University, Yangling 712100, China
[c] Institute of Soil and Water Conservation, Chinese Academy of Sciences and Ministry of Water Resources, Yangling 712100, China

ARTICLE INFO

Handling Editor: David Laird

Keywords:
Biochar
Surface charge
Aggregate breakdown
Particles interaction
Hamaker constant

ABSTRACT

Biochar amendments are effective for stabilizing soil aggregates and improving the quality and fertility of soils. Soil internal forces (SIFs), including electrostatic, hydration, and van der Waals forces, can substantially affect aggregate stability; however, there has been relatively little focus on the effects of biochar addition on SIFs and their relation to aggregate stability. In this work, in order to quantitatively investigate the influence of biochar on aggregate stability, we collected soil samples with different biochar application rates (0, 2.5%, 5.5%, and 7.0%; w/w) after a two-year field experiment, and then used Na^+-saturated soil aggregates (1–5 mm) to conduct our experiments. Our results demonstrated that after 2-year, specific surface area (SSA), soil organic carbon (SOM), cation exchange capacity (CEC), and surface charge density (σ_0) increased while soil pH slightly decreased with biochar application from 0% to 7%. Soil aggregate stability increased with the biochar application rate. Theoretical calculations indicated that forces of electrostatic repulsion and van der Waals attraction both increased in response to biochar incorporation, however the net pressure of SIFs decreased. Soil aggregate stability was well explained by the theoretical calculations. Biochar addition reduced the net pressure of SIFs and stabilized soil aggregates. Overall, the investigation by using the mono-cationic model system showed that SIFs played important roles in the aggregate stability and explained well the aggregate stability of amended soils. The findings of this work initiate the process of elucidating and quantifying the complex biochar-mineral interaction mechanism in soil systems.

1. Introduction

Aggregates are considered one of the basic functional units of soils. Aggregate stability affects numerous soil properties and processes including carbon and nitrogen cycling, emission of greenhouse gas, nutrient storage and transport, water infiltration, tilth, and soil erosion (Tisdall and Oadcs, 1982; Six et al., 2000; Van Oost et al., 2007; Rabot et al., 2018). Therefore, aggregate stability is vital for agricultural productivity and environmental quality (Amézketa, 1999; Bronick and Ral, 2005; Rabot et al., 2018), and the improvement of aggregate stability is a major objective of soil management.

Heating biomass under limited oxygen condition leads to the formation of biochar. Biochar is an organic porous material containing high carbon contents (Sohi et al., 2010; Alwabel et al., 2018). Biochar amendment is highly advantageous for the soil as it is responsible for better soil quality, crop productivity and environmental health (Lehmann, 2007; Spokas et al., 2009; Sohi et al., 2010; Arif et al., 2017; Gao et al., 2019; Luo et al., 2020; Zhang et al., 2020b). Field and laboratory trials demonstrate that biochar amendments can promote soil aggregation and stabilization of aggregates (Mukherjee and Lal, 2013; Herath et al., 2013; Lu et al., 2014; Liu et al., 2014; Fungo et al., 2017; Zhang et al., 2020a). Wang et al. (2017) reported that soil aggregation was enhanced in a fine-textured Yolo soil after the addition of biochar. Biochars based on softwood and walnut shell improved soil aggregation by 217% and 126%, respectively. The study of Peng et al. (2011) showed that biochar made from rice straw was ineffective for improving aggregate stability in an Ultisol of southern China. Similar observations for temperate soils have also been described by Liu et al. (2014) and

* Corresponding author at: No. 26, Xinong Road, State Key Laboratory of Soil Erosion and Dryland Farming on the Loess Plateau, Northwest A&F University, Yangling 712100, China.
E-mail address: fbzhang@nwsuaf.edu.cn (F. Zhang).

https://doi.org/10.1016/j.geoderma.2021.115276
Received 16 March 2021; Received in revised form 28 May 2021; Accepted 2 June 2021
Available online 22 June 2021

Borchard et al. (2014). However, Burrell et al. (2016) conducted a pot experiment using woodchip biochar and studied its long-term effects on a Cambisol, a coarse-textured Planosol, and Chernozem. They reported stronger ability of biochar to stabilize the soil aggregates in the Planosol than the Cambisol and no affect for the Chernozem. From a one-year biochar amendment study on a sandy soil, Zhang et al. (2015) reported that the amendment was ineffective towards soil aggregation or aggregate stability. Despite substantial research effort, a clear pattern of biochar effects on aggregate stability has not emerged, because of the great variations in soil property, biochar quality, and environmental conditions that can affect the response of aggregate stability (Mukherjee and Lal, 2013; Herath et al., 2013; Lychuk et al., 2014; Zhao and Zhou, 2019). Therefore, further research should be conducted to elucidate the mechanisms underlying the biochar effects on soil aggregate stability.

The stability of soil aggregates in water is controlled mainly by soil internal forces (SIFs), i.e. van der Waals attraction, hydration and electrostatic forces (Farres, 1980; Hu et al., 2015; Rengasamya et al., 2016; Yu et al., 2020). In theory, two adjacent soil particles exhibit internal forces that can be equivalent to hundreds of thousands of atmospheres (Li et al., 2013; Huang et al., 2016; Ding et al., 2019). It was proposed that SIFs have a stronger influence on aggregate stability than other factors like raindrop impact, and slaking (Farres, 1980; Hu et al., 2015; Yu et al., 2020). These forces are the results of interactions between the electrically charged soil particles and/or water molecules in bulk solution (Quirk, 1994; Bolan et al., 1999; Rengasamya et al., 2016). Thus, the interactions of soil particles are dependent on their surface electrochemical properties such as surface charge density (σ_0), specific surface area (SSA), surface potential, and cation exchange capacity (CEC), and environmental conditions (e.g., electrolyte concentration and ion species of soil solution, and pH) (Hu et al., 2018a, 2018b; Liu et al., 2020). Thus, factors influencing soil electrochemical properties could have important effects on the internal forces and further the stability of soil aggregates (Xu et al., 2015; Yu et al., 2020).

Biochar addition can alter many soil physicochemical properties. Biochar possesses large surface areas with multiple charged functional groups capable to interact with soil minerals (Sohi et al., 2010; Zhao et al., 2015; Palansooriya et al., 2019; Zhao and Zhou, 2019). Biochar-mineral interactions can promote biochar oxidation and create new functional moieties on its surface, such as –COOH and –OH which facilitate the biochar-mineral complex formations (Glaser et al., 2000; Qian and Chen, 2014; Zhao and Zhou, 2019). Many studies showed that biochar incorporation enhances the SSA and CEC of soil because of the complex formation between soil minerals and biochar (Mukherjee et al., 2011; Alwabel et al., 2018; Palansooriya et al., 2019). The classic double layer theory suggests that changes in CEC and SSA can modulate the soil interaction forces which further exhibit a great effect on aggregate stability (Huang et al., 2016, Yu et al., 2020). However, to our knowledge, there are few studies on how biochar influences soil internal forces through modifying soil surface properties and their effects on aggregate stability. Therefore, exploring the quantitative information regarding biochar impact on aggregate stability in terms of particle-solution interactions and derived SIFs is important for clarifying the underlying mechanism of how biochar stabilizes soil aggregates.

The main objective of this study is to quantify the effects of biochar amendment on SIFs and aggregate stability, as well as to explore the mechanisms underlying these responses. Due to the inherent complexity of natural soil system (e.g., various ion types and uncertain electrolyte concentration in soil solution), the quantitative calculation of internal forces of natural soils is still challenging in practice. Therefore, to investigate the influence of biochar on soil aggregate stability in a quantitative manner, we collected soil samples with different biochar application rates (0, 2.5%, 5.5%, and 7.0%) from a two-year field study, and evaluated the aggregate stability under a carefully designed monocationic model system with the aim to make theoretics predictions based on the soil surface properties and the classic diffuse double layer model (Yu et al., 2017; Xu et al., 2015). In doing so, we can exclude the influences of other environmental conditions (e.g., ion types and concentration in bulk solution) and directly gain the quantitative information of SIFs and their effects on aggregate stability of biochar-amended soils.

2. Materials and methods

2.1. Biochar

The biochar used in this research was derived from clipped apple branches as the study area is a major apple-producing region in China. The apple branches were pyrolyzed at 550 °C and the carbonized material was allowed to pass through a 2-mm sieve before field application. The biochar contained 332 g kg^{-1}C, 3.33 g kg^{-1}N, which were quantified using a Vario EL cube elemental analyzer (German Element, GRE). It had a specific surface of 9.95 m^2 g^{-1}, determined by N_2 adsorbtion at 77 K with a V-Sorb 2800P SSA (GAPP, CHN); CEC of 2.3 cmol kg^{-1}, measured by the ammonium acetate exchange method; pH of 8.75 (1:15, w/v) by measuring the mixture after 24 h shaking and standing for 1 h using a pH meter.

2.2. Field experimental setup

We conducted the field experiment at the long-term Ansai field experiment station which was established in 1973 and located in the northern Loess Plateau in Shaanxi Province (109°19′23″ E 36°51′30″ N). The annual average precipitation of this site is 500 mm and an average temperature of 8.8 °C (Li et al., 2019). According to the FAO (Food and Agriculture Organization) soil classification, the soil of this site is a Calcic Cambisol. The main clay minerals of the soil were illite (~40%), kaolinite (~20%), chlorite (~20%), montmorillonite (~10%) and vermiculite (~5%) (Hu et al., 2018a). The soil texture consisted of 8.0% clay, 53.9% silt and 38.1% sand, and is classified as a silt loam based on the U.S. Department of Agriculture definitions. Soils in this region usually have low organic matter content and suffer from serious erosion. The soil used in this study had organic matter content of 5.8 g kg^{-1} and pH of 8.25 before the biochar amendment.

The field experiment was established in August 2017. The biochar was evenly spread across the soil by raking and incorporated into the soil to ~20 cm depth. We chose four application rates as treatments: 0%, 2.5%, 5.5%, and 7.0% (w/w) and each was replicated three times. The experiment comprised of 12 subplots, each of which had an area of 6 m^2 (4 × 1.5 m). During the field study, we removed the weeds in the experimental plots occasionally so as to minimize any over growth of vegetation.

2.3. Sampling and analysis of soil

The collection of soil samples was carried out in August 2019, 24 months after the biochar amendment. We randomly collected three soil cores per micro-plot at 0–10 cm depth, composited as a single soil sample. After the soil samples were air-dried and visible matter (plant roots, stones, and debris) was removed, samples were stored in individual plastic bags. Soil samples ~1.0 kg were transferred to the laboratory for further analysis. Prior to determine the soil properties, the free biochar particles in the soil samples were removed by flotation in distilled water.

Determination of soil pH was conducted with a pH meter using a soil : water ratio of 1:2.5. The $K_2Cr_2O_7$ oxidation method was used for determining SOC content (Kalembasa and Jenkinson, 1973). Soil CEC, SSA, and surface charge density (σ_0) were measured by the surface property determination protocol proposed by Li et al. (2011). In brief, soil samples were H-saturated in advance, and followed by exchange equilibrium experiments using the mixture solution of NaOH and Ca$(OH)_2$; finally the Na^+ and Ca^{2+} concentrations in the supernatant were measured and the CEC, SSA, and σ_0 were calculated based on the double

layer theory. The detailed steps can be found in our recent study (Liu et al., 2020). The water stability of soil aggregates characterized by mean weight diameter (MWD) was evaluated by a modified wet sieve method (Zhang et al., 2019), except that the diameter of soil aggregates was 1–5 mm, and we did the experiment manually in the present study. All the above mentioned soil properties were measured in triplicate, and average values were used for data analysis.

2.4. Soil aggregate preparation and stability determination

Due to the complexity of natural soils, quantification of soil internal forces is still challenging in practice. Thus, to quantitatively evaluate the effect of biochar on soil internal forces, Na^+-saturated soil aggregates were used in the following study. According to the reported literature (Xu et al., 2015; Li et al., 2015), Na^+ weakly polarizes at the soil colloid interface, and is, therefore, appropriate to evaluate the soil internal force effect on aggregate stability. Here, we used the protocol of Xu et al. (2015) to prepare Na^+-saturated soil samples. In a 5-L beaker, about 800 g of biochar amended soil sample was dispersed in 4 L of 0.5 M NaCl solution by agitation, followed by centrifugation and decantation. The process was repeated three times. To remove the excess Na^+ from the bulk solution, soil samples were washed with 4 L of deionized water through centrifugation and decantation three times, followed by oven dried at 60 °C. They were then crushed manually and passed through sieves to obtain re-form aggregates of 1–5 mm diameter. Here, Na^+-saturated soil aggregates were representative of simplified soil systems which can let us directly calculate the internal forces of all soil samples under given environmental conditions.

Soil aggregate breaking strength (w %) was employed to evaluate its aggregate stability (Yu et al., 2017). It was defined as the percent of a mass release in the form of fine particles with diameters < 20 and < 10 μm after macroaggregates breakdown. As the percent mass release increases, soil aggregate stability decreases. Specifically, in 4 cylinders (500 mL), NaCl solution of different concentrations (1, 10^{-1}, 10^{-2}, and 10^{-4} M) were prepared, followed by the addition of 10 g of Na^+-saturated soil aggregates of 1–5 mm in diameter. After 2 min, the cylinders were gently inverted four times within the next 2 min. After the onset of precipitation, the pipette method based on the Stokes law was utilized to investigate the mass percent of the particles released (<20 μm and < 10 μm) in the total mass of aggregate (w (<d) %). The detailed steps were also given in the previous studies (Xu et al., 2015). Here, we tested aggregate stability under a given electrolyte solution (1-10^{-4} M NaCl solution), because varying the environmental conditions can affect soil electrostatic forces between soil particles; and it also simulated the drying and wetting cycles of soils, which could change the ion concentration in soil bulk solution.

2.5. Quantification of soil internal forces

Soil internal forces include electrostatic, van der Waals and hydration forces. Changes of soil properties could results in different soil internal forces, especially electrostatic, and van der Waals forces. According to the classic double layer theory, the parameters of soil CEC and SSA can greatly affect the electrostatic repulsive force between soil particles.

The electrostatic repulsive pressure (P_{ele}) existing between soil particles can be calculated as (Li et al. 2013):

$$P_{ele} = \frac{2}{101} RTc_0 \left\{ cosh\left[\frac{ZF\phi(d/2)}{RT}\right] - 1 \right\} \quad (1)$$

where Z is the cation valence, R (J·mol^{-1}·K^{-1}) is the gas constant, c_0 (mol L^{-1}) is the equilibrium bulk solution cation concentration, d (dm) is the distance between two adjacent particles, F (C mol^{-1}) is Faraday's constant, T (K) is the absolute temperature, and $\varphi(d/2)$ (V) is the potential at the middle of the overlap of the electric double layers of two adjacent particles. $\varphi(d/2)$ (V) may be calculated as follows:

$$\frac{\pi}{2}\left[1 + \left(\frac{1}{2}\right)^2 e^{\frac{2ZF\varphi(d/2)}{RT}} + \left(\frac{3}{8}\right)^2 e^{\frac{4ZF\varphi(d/2)}{RT}}\right] - arcsine^{\frac{ZF\varphi_0 - ZF\varphi(d/2)}{2RT}} = \frac{1}{4}d\kappa e^{\frac{-ZF\varphi(d/2)}{2RT}} \quad (2)$$

where κ (1/dm) is the Debye–Hückel parameter. For 1:1 electrolytes, $\kappa=(8\pi F^2 c_0/\varepsilon RT)^{1/2}$ and φ_0 (V) is the particle surface potential. Here, the soil surface potential for a 1:1 type electrolyte is calculated as follows (Li et al., 2004):

$$\varphi_0 = -\frac{2RT}{ZF} ln\left(\frac{1-a}{1+a}\right) \quad (3)$$

in which

$$\frac{\kappa C_T}{Sc_0} = 1 + \frac{4}{1+a} - \frac{4}{1+e^{-1}a} \quad (4)$$

$$\kappa = \sqrt{\frac{8\pi F^2 Z^2 c_0}{\varepsilon RT}} \quad (5)$$

where S (m^2 g^{-1}) is the specific surface area, C_T (mol·g^{-1}) is the cation exchange capacity, S and C_T are the average values for the soil; ε is the dielectric constant for water, and a is the intermediate variable.

The van der Waals force is closely related to the effective Hamaker constant (A_{eff}) which is the inherent property and depends on the material composition of soil. This means that different biochar addition in our study could lead to different A_{eff} values and thus the van der Waals force between soil particles. The van der Waals attractive pressure (P_{vdw}) can be calculated from the following equation (Yu et al., 2017):

$$P_{vdw} = -\frac{A_{eff}}{0.6\pi}(10d)^{-3} \quad (6)$$

where A_{eff} (J) is the effective Hamaker constant, and here A_{eff} is the average value for the soil. A_{eff} (J) was estimated by analyzing the dry end of the soil water characteristic curves with a dew point potentiometer (WP4-T; Decagon Devices, Pullman, WA, USA). The determination was based on the protocol of Tuller and Or (2005). Thus, A_{eff} could be estimated as follows:

$$\theta m = -\rho_w \times S \times \left(\sqrt[3]{\frac{Aeff}{6\pi\rho_w g\psi}}\right) \times 1000 \quad (7)$$

where θ_m (kg kg^{-1}) is the gravimetric water content while g (m s^{-2}) is the gravitational acceleration, ρ_w (kg m^{-3}) is the density of water, and ψ (m H_2O) is the matrix potential head. Detailed determinations for A_{eff} resembled with those reported by Yu et al. (2017). Here, according to the Equation (7), we fitted the relationship between matric potential and gravimetric water content for various biochar containing soils (Fig. S1). Therefore, we can obtain that A_{eff} for soils with application rates of biochar in 0.0%, 2.5%, 5.5%, and 7.0% were 6.44×10^{-20}, 7.75×10^{-20}, 9.43×10^{-20}, and 1.09×10^{-19} J, respectively.

The hydration repulsive pressure can be estimated from the following equation (Li et al., 2013):

$$P_h = 3.33 \times 10^4 e^{-5.76 \times 10^9 d} \quad (8)$$

where P_h (atm) is the surface hydration pressure, d (dm) is the distance between two adjacent soil particles.

3. Results

3.1. Effects of biochar on natural soil properties

Table 1 lists soil properties under various biochar application rates after two years of the field experiment. As can be seen from this table, soil pH became reduced with increasing biochar addition. SOC contents

Table 1
The properties of natural soils under different biochar application rates.

Biochar (%)	pH	SOC (g^{-1} kg^{-1})	CEC (cmol kg^{-1})	SSA (m^2 g^{-1})	σ_0 (C m^{-2})	MWD (mm)
0.0	8.25 ± 0.06d	1.74 ± 0.35a	5.78 ± 0.00a	20.26 ± 0.40a	0.275 ± 0.004a	0.434 ± 0.040a
2.5	8.18 ± 0.03c	8.80 ± 1.14b	6.95 ± 0.03b	23.92 ± 0.21b	0.280 ± 0.002a	0.650 ± 0.059b
5.5	8.11 ± 0.04b	19.07 ± 1.04c	7.93 ± 0.08c	25.90 ± 1.93bc	0.296 ± 0.019ab	0.774 ± 0.040c
7.0	7.99 ± 0.01a	23.19 ± 0.81d	8.86 ± 0.09d	27.76 ± 1.15c	0.308 ± 0.014b	1.248 ± 0.026d

Notes: SOC, soil organic carbon; CEC, cation exchange capacity; SSA, specific surface area; σ_0, surface charge density; MWD, mean weight diameter. Values are means ± standard deviation. Different lowercase letters indicate significant differences between different biochar application rates at $p < 0.05$ (n = 3).

increased from 1.71 to 37.04 g^{-1} kg^{-1} as the rate of biochar application increased from 0 to 7.0%. Similar to SOC contents, the soil surface electrochemical properties, the CEC, SSA, and σ_0, increased by 53.4%, 37.1%, and 12.0%, respectively, as the biochar application rate increased from 0 to 7.0%. The MWD significantly increased (from 0.466 to 1.277 mm) with the increasing biochar application rate (from 0 to 7.0%; $p < 0.05$).

3.2. Effects of biochar on soil internal forces in Na^+-saturated aggregates

3.2.1. Electrostatic pressure between soil particles

To obtain the electrostatic pressure between soil particles, we chose a simplified system of Na^+-saturated aggregates of biochar-amended soils to directly calculate the electrostatic pressure between soil particles while varying the electrolyte concentration in bulk solution. Here, the positive values represent the repulsive pressure that could cause soil aggregates break down. From Equations (1) to (5) and the values of CEC and SSA in different biochar-added soils (Table 1), and the electrolyte concentrations in bulk solution (c_0), which varied from 1 to 10^{-4} M, the electrostatic repulsive pressure between soil particles can be estimated (Fig. 1). The electrostatic repulsive pressure differed among the various biochar amendments (Fig. 1), which increased with the increasing biochar application rates (from 0 to 7%). To clearly analyze their effects,

Table 2
Electrostatic repulsive pressure (P_{ele}, atm) at 2 nm between soil particles and under various bulk solution electrolyte concentrations and biochar application rates.

Electrolyte concentration(mol L^{-1})	Biochar application rate (%)			
	0.0	2.5	5.5	7.0
1	0.72	0.73	0.76	0.79
0.1	13.74	13.81	13.99	14.13
0.01	17.42	17.49	17.70	17.85
0.001	17.76	17.84	18.05	18.21
0.0001	17.78	17.85	18.07	18.23

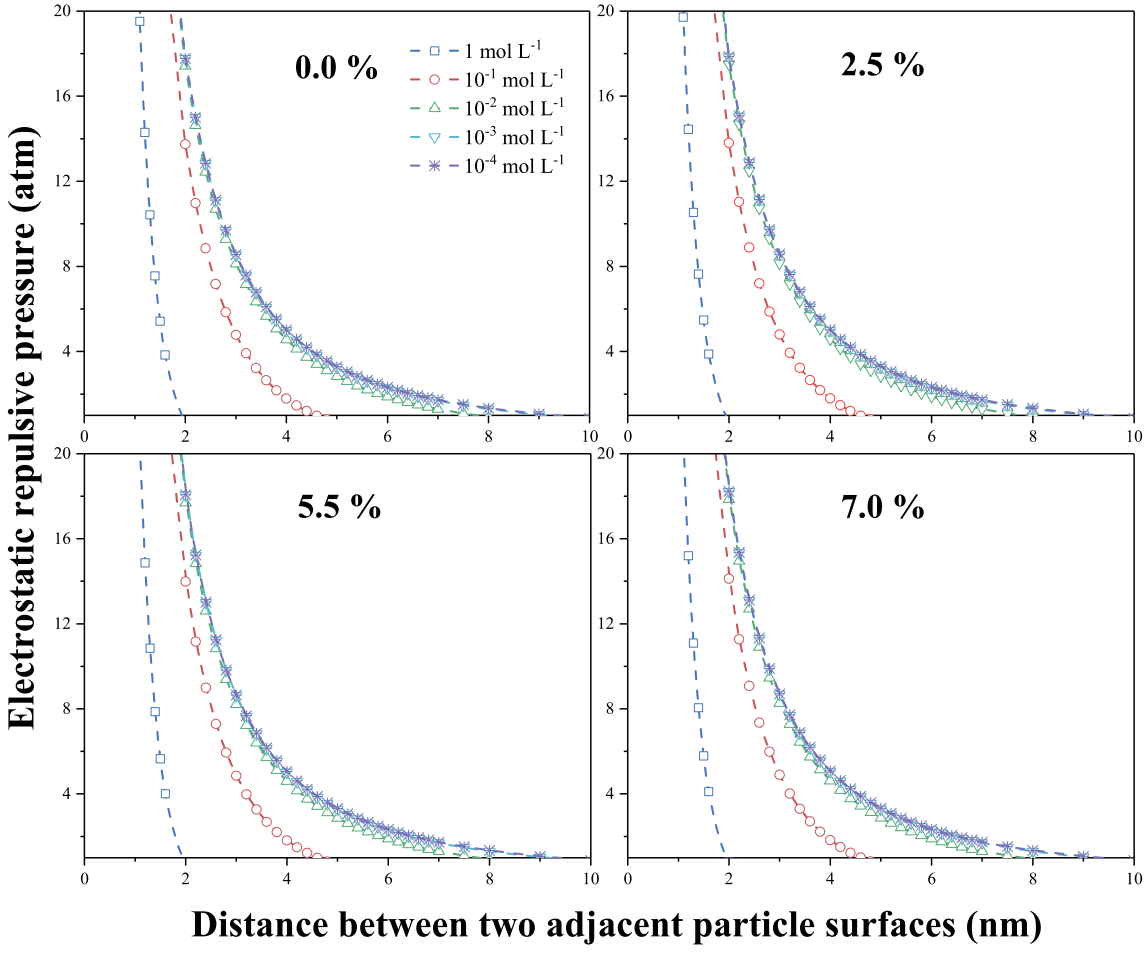

Fig. 1. Distribution of electrostatic repulsive pressure between two adjacent soil particles at various bulk solution electrolyte concentrations; biochar addition rates: 0%, 2.5%, 5.5%, 7.0%.

Table 2 lists the electrostatic repulsion pressures for biochar-amended soils at the distances of 2 nm between soil particles under various electrolyte concentrations. The results indicate that the pressure of electrostatic repulsion increases with the biochar application rate. For the given treatments, electrostatic repulsion rapidly increased with decreasing the bulk solution electrolyte concentration from 1 to 10^{-2} M and then increased slowly and finally leveled off for the two lowest concentrations. Therefore, the critical electrolytic concentration is 10^{-2} M that is capable of changing the electrostatic repulsion. In addition, electrostatic repulsion decreased with increasing distance between soil particles and the concentration of electrolytes.

3.2.2. The van der Waals and surface hydration pressures between soil particles

Here, the negative values represent the attractive pressures that stabilize soil aggregates. According to the Equations 6–7, and 8, the van der Waals and surface hydration pressure can be derived. Fig. 2 shows the distribution of van der Waals and surface hydration pressures. The biochar application enhanced the attraction of van der Waals in soil particles. For two adjacent particles at 1.4 nm apart, the van der Waals attractive pressure were −12.5, −15.0, −18.2, and −21.2 atm in soils with the application rates of 0.0%, 2.5%, 5.5%, and 7.0%, respectively. As the distance between soil particles increased, the force of surface hydration repulsion decreased. The force of repulsion would be dominant over an attractive force for the soil particle separation of <1.4 nm. The difference between the forces of van der Waals and the surface hydration sharply increased with decreasing space between soil particles. Hence, whenever dried soil aggregates are wetted the repulsive pressure generally overcomes van der Waals attractive pressure.

3.2.3. Net pressure between soil particles

To understand the overall changes of soil internal forces, we further evaluated the soil net pressure which is the sum of electrostatic, van der Waals and surface hydration pressures between soil particles. Fig. 3 shows the net pressure distribution between two adjacent particles of biochar-amended soils at various electrolyte concentrations. The particles separated by 2 nm exhibited a net attractive pressure at a 1 M electrolyte concentration. Strong repulsive pressures occurred at all electrolyte concentrations when the particles were < ~1.5 nm distance. With the decrease in bulk electrolyte concentration, the net pressure would increase and overlap at electrolyte concentrations ≤ 10^{-2} M. Thus, 10^{-2} M was the critical bulk solution electrolyte concentration.

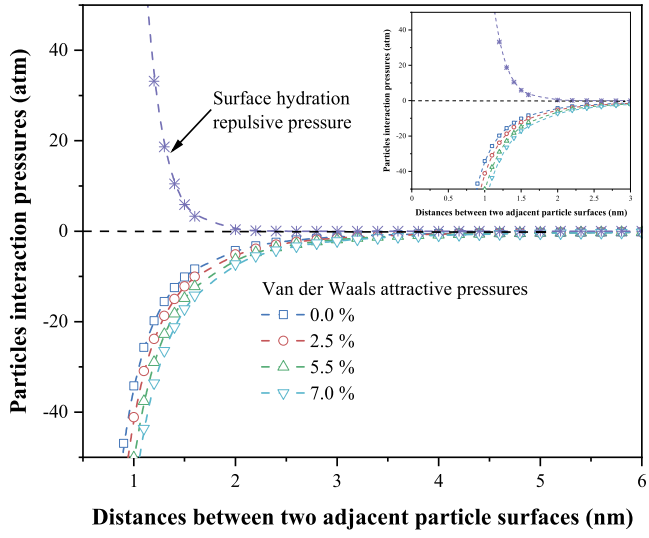

Fig. 2. Distributions of van der Waals attractive pressure and surface hydration repulsive pressure.

Biochar application altered the net pressure of soil particles (Fig. 3). For the determination of the impact of biochar amendment on the net pressure exhibiting by two adjacent particles, the relationships between the net pressure at 2 nm soil particle distance and the electrolyte concentration were plotted (Fig. 4). For each electrolyte concentration and distance between soil particles, the net pressure declined with increasing rate of biochar application. For all the treatments, decreasing electrolyte concentration from 1 to 10^{-2} M results in increasing the net pressure and the pressure reached a plateau with a further decrease in the concentrations of electrolyte from 10^{-2} to 10^{-4} M. Therefore, the critical electrolyte concentration was 10^{-2} M. Each treatment exhibited net attractive pressure at 1 M concentration of electrolyte.

3.3. Effects of biochar on Na^+-saturated aggregates stability

To investigate the effects of soil internal forces on aggregate stability, the aggregate breaking strength of biochar-amended soils under given electrolyte concentration was measured and the results are shown in Fig. 5. Breaking strength decreased with increasing biochar application rate for each electrolyte concentration. Hence, soil aggregate stability increased with the biochar amendment level. Similarly, the breaking strength became enhanced when the concentration of electrolyte in the bulk solution decreased. i.e. by decreasing the concentration from 1 to 10^{-2} M, the breaking strength of soil aggregates logarithmically increased. In contrast, the soil aggregate breaking strength reached steady-state at electrolyte concentrations < 10^{-2} M. Hence, it was the critical point for the breakdown of soil aggregates.

3.4. Relationship between soil internal forces and Na^+-saturated aggregate stability

To further quantitatively analyze the effects of soil internal forces on aggregate stability, we directly established the relationship between the net pressure at 2 nm soil particle distance and aggregates breaking strength of biochar-amended soils (Fig. 6). The distance of 2 nm was chosen, because the hydration repulsive pressure can be ignored, and the electrostatic pressure has been shown to be the main force inducing aggregates explosion in aqueous system (Li et al., 2013). The soil aggregate breaking strength had positive correlations with the net pressure at 2 nm between soil particles. There were significant exponential relationships between aggregates breaking strength (<10 and 20 μm) of the whole biochar-amended soils and the net pressure of soil particles, indicating that soil aggregate stability decreased exponentially as the net pressure of soil particles increased, and increased as the biochar application rates increased.

4. Discussion

4.1. Responses of soil properties to biochar application

Biochar application remarkably affects the soil physicochemical properties. It can enhance the quality and fertility of the soil (El-Naggar et al., 2019; Zhang et al., 2020b). Our results showed that biochar slightly but consistently lowered soil pH (Table 1). Previous studies also reported a similar minor decrease in soil pH after incorporation biochar into the soils having alkaline pH (Liu and Zhang, 2012; Lentz and Ippolito, 2012; Abrishamkesh et al., 2015; Laghari et al., 2015; Zhang et al., 2020b). Nevertheless, the outcome of the present work did not agree with some other studies that reported the liming impacts of biochar after its amendment in soils of acidic nature. After biochar incorporation, the possible change in pH varies with soil and biochar type, biochar quantity, and environmental conditions (El-Naggar et al., 2019). The decline noted in soil pH upon the incorporation of biochar in our study could be explained as follows: (1) biochar oxidation (aging) in soils can promote the production of phenolic and carboxylic acids that reduce soil alkalinity (Cheng et al., 2006; Zhang et al., 2020b) and (2)

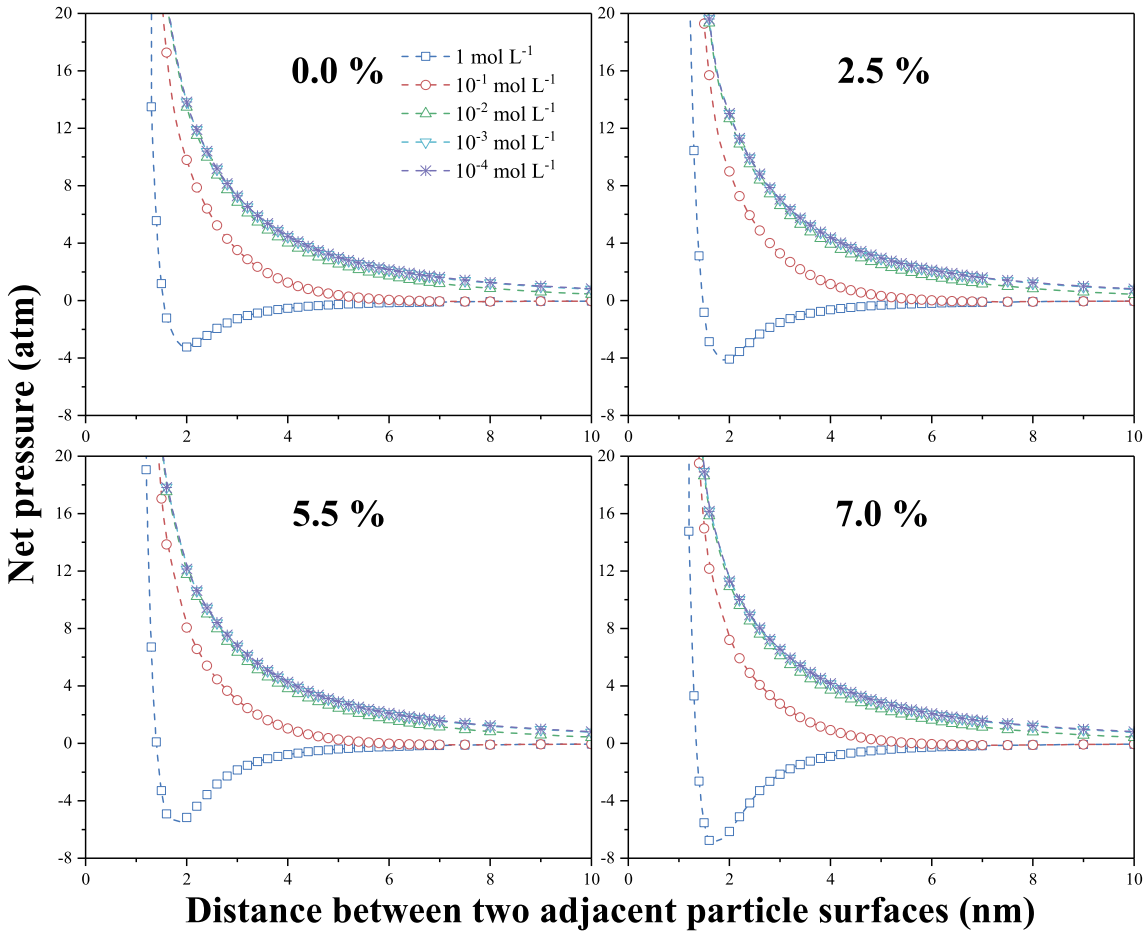

Fig. 3. Net pressure distribution of two adjacent soil particles at various bulk solution electrolyte concentrations.

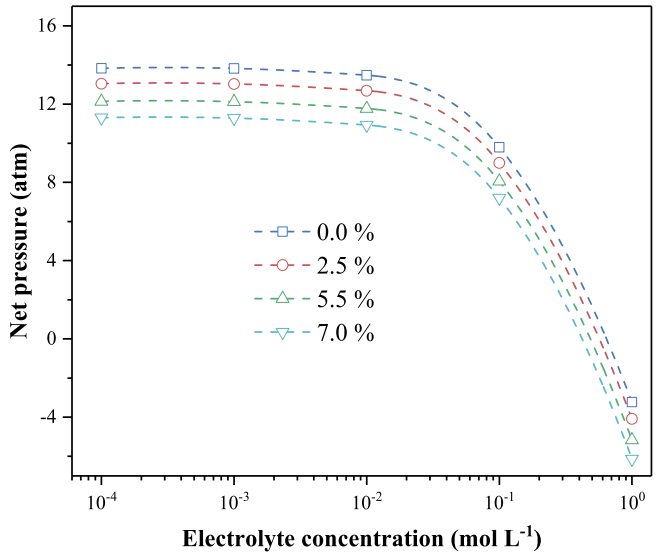

Fig. 4. Net pressure at 2 nm between soil particles and in various bulk solution electrolyte concentrations.

biochar addition could improve the buffering capability of soil pH (Xu et al., 2012).

Biochar application is capable of enhancing SOC sequestration (Mukherjee and Lal, 2013; Wang et al., 2016; El-Naggar et al., 2019). Many previous studies have shown that an increase in SOC is a direct consequence of the biochar amendment (Sohi et al., 2010; Alwabel et al., 2018), which is confirmed in this study (Table 1). This can be explained by the fact that biochar has a high C content; and its microbial degradation furnishes recalcitrant aromatic C. For these reasons, prolonged biochar amendment can thus increase SOC and improve aggregate stability (Purakayastha et al., 2015; El-Naggar et al., 2015, 2019; Wang et al., 2016). In addition, many studies have found that the biochar amendment ameliorates soil structure, increases soil aggregate stability, and physically protects SOM against rapid decomposition (Zhang et al., 2015, 2020a, 2020b; Wang et al., 2017; Luo et al., 2020).

Many studies suggested that the incorporation of biochar was capable of increasing CEC, SSA, and σ_0 of soil (Mukherjee and Lal, 2013; Alwabel et al., 2018; Palansooriya et al., 2019; El-Naggar et al., 2019). Yuan and Xu (2011) reported that biochar incorporation increases the CEC of acid soils of subtropical and tropical China having relatively low initial CEC. Laird et al. (2010) reported the increase in SSA of biochar-amended soils with application rate from 0.0% to 2.0%. Liang et al. (2006) reported that the Anthrosols from the Brazilian Amazon had comparatively higher CEC, SSA, and σ_0 than adjacent forest soils as the former had higher black carbon content. Liu et al. (2020) indicated that organic matter enrichment during the restoration of vegetation significantly improved the CEC, SSA, and σ_0 of loessial soil. Hence, organic material inputs have dramatic effects on soil surface properties. Our results also showed that biochar application improved soil CEC, SSA, and σ_0 and their values increased with biochar application rates (Table 1). Biochar amendment can enhance soil surface properties as the material has a wider pore size distribution and high surface area (Chan and Xu, 2009; Mukherjee et al., 2011). Besides, it is quite important that biochar undergoes various physical and biochemical reactions in the soil

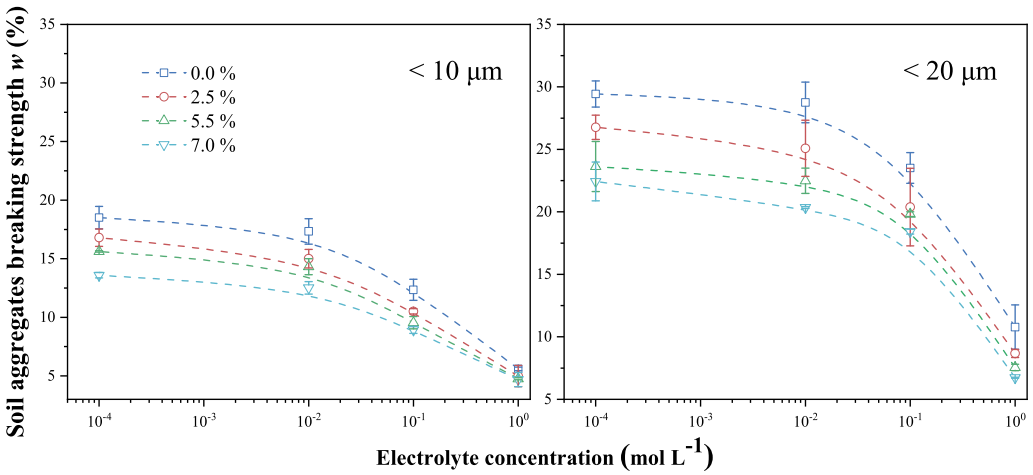

Fig. 5. Relationship of soil aggregate breaking strength with bulk solution electrolyte concentration. Error bars represent the standard error of the mean (n = 3).

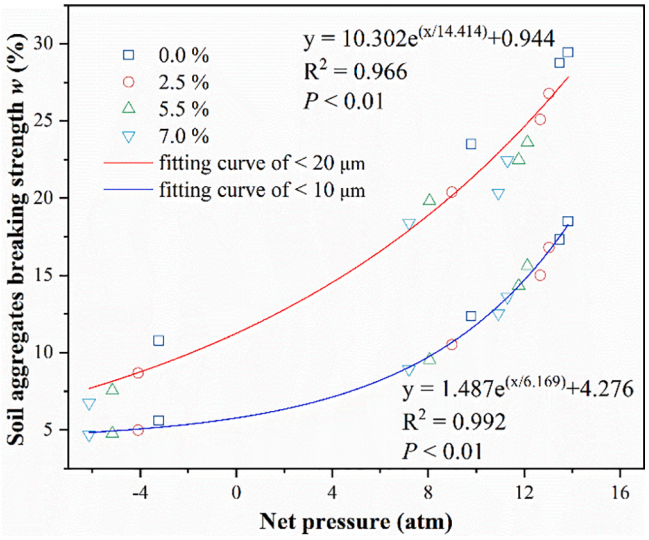

Fig. 6. Relationship between the net pressure at 2 nm soil particle distance and aggregates breaking strength of biochar-amended soils.

(Zhao and Zhou, 2019). Natural biochar oxidation can generate carboxyl groups that improve soil surface properties (Liang et al., 2006; Suddick and Six, 2013). Cheng et al. (2008) stated that the oxygen-bearing functional moieties on the biochar-mineral complexes formed during biochar aging have surface negative charges that increase with biochar oxidation.

4.2. Responses of soil internal forces to biochar application

The interactive forces between soil particles are largely affected by soil intrinsic and extrinsic factors including CEC, SSA, σ_0, solution composition and concentration, pH, and others (Huang, 2004; Li and Xu, 2008; Rengasamy et al., 2016). Here, negative pressure indicates attraction between soil particles while positive pressure represents repulsion. Our study reveals the electrostatic repulsive pressures between soil particles increased with biochar application at each electrolyte concentration (Table 2). This finding agrees with that reported by Yu et al. (2017). The results can be explained by increased soil surface charge density after biochar incorporation (Table 1) (Li and Xu, 2008; Xu et al., 2020). Meanwhile, the soil electrostatic repulsive force increased with decreasing bulk solution electrolyte concentration (Fig. 1; Table 2). This result was also described by the previous literature (Gong et al., 2018; Ding et al., 2019). According to the classic double layer theory, elevated bulk solution electrolyte concentration compresses the double soil colloid layer, thereby reducing the electrostatic repulsive force of soil particles or vice versa (Liang et al., 2007). Therefore, this result indicates that biochar addition and the decreasing electrolyte concentration could both increase soil electrostatic force between soil particles. The result also suggests that when rain penetrates the soil, the bulk solution electrolyte concentration is lowered by dilution leading to an increase in the electrostatic repulsion between soil particles.

In this study, the van der Waals attractive force was found stronger upon biochar incorporation after two years field study. Specifically, the van der Waals force increases with the biochar application rate (Fig. 2), indicating that biochar application could increase the attractive force between soil particles offsetting the increased electrostatic repulsion force. Earlier studies reported similar findings (Yu et al., 2017, 2020). Yu et al. (2020) found that in Vertisols and Ultisols, the van der Waals force decreased in response to SOM removal but increased after straw incubation (SOM addition) as compared to control. The main reason can be attributed to the increase of the soil Hamaker constant (A_{eff}) as the biochar amended into soils (Eq. (6)). A_{eff} represents the average interactions between macroscopic bodies and liquids caused by short-range van der Waals forces. This constant depends on the properties of the materials showing interaction with each other and the intervening media (Ackler et al., 1996; Bergstrom, 1997). Here, we found that the soil A_{eff} at the 0.0%, 2.5%, 5.5%, and 7.0% biochar application rates were 6.44×10^{-20}, 7.75×10^{-20}, 9.43×10^{-20}, and 1.09×10^{-19} J, respectively. Thus, biochar addition increases soil A_{eff} which reflects in the increasing van der Waals attractive force between soil particles. In an earlier study, theoretical calculation revealed that the A_{eff} of Lou soil, classified as Calcic Cambisols according to FAO soil classification and developed from the same parent materials as the soils studied here, decreased from 6.86×10^{-20} to 3.14×10^{-20} J with the SOM removal (Wang et al., 2020). Determination of exact soil Hamaker constant is quite difficult because the surface geometry is complex and the solid phase is heterogeneous. Typical soil Hamaker constants are in the range of -10^{-19} to 10^{-20} J (Watanabe and Mizoguchi, 2002; Tuller and Or, 2005), which agreed with our present study. Moreover, biochar amendment increases soil A_{eff} mainly because clay form complexes with organic matter (Resurreccion et al., 2011). Therefore, our results suggest that biochar addition can increase van der Waals attraction between soil particles as indicated by increasing soil A_{eff}.

Our study showed that the net pressure exhibited by SIFs decreased by increasing the biochar application rate (Fig. 4). Hence, biochar addition reduces net repulsive forces between soil particles. This result resembles those reported by Yu et al. (2017). They stated that the

increase in SOM caused by straw incubation reduces the net pressure of soil comprising the sum of SIFs. Biochar addition increased both electrostatic repulsion and van der Waals attraction forces; but the increased attraction forces offset the increased electrostatic repulsive force (Table 2; Fig. 2) and thus improving soil aggregate stability.

4.3. Responses of soil aggregate stability to biochar application

The present study showed that soil aggregate breaking strength decreased with increasing biochar application rate (Fig. 5), indicating that soil aggregate stability improved with biochar addition. This result based on the Na^+-saturated aggregates were in line with that of natural soil aggregates (Table1, MWD). Several studies showed the positive impact of biochar on soil aggregate stability both in the field and laboratory studies (Liu et al., 2014; Hartley et al., 2016; Fungo et al., 2017; Wang et al., 2017; Zhang et al., 2020a, 2020b). The increase in SOC after biochar incorporation could improve aggregate stability (Six et al., 2004; Ojeda et al., 2015; Wang et al., 2016; Alwabel et al., 2018). SOM is an important soil binding agent. Its increase after the biochar amendment facilitates the formation as well as stability of soil aggregate (Haynes and Naidu, 1998; Soinne et al., 2014; Omondi et al., 2016; El-Naggar et al., 2019). However, the mechanism underlying this process is complex and poorly understood (Wang et al., 2017). Natural biochar oxidization produces hydroxyl and carboxylic functional groups that promote soil particle and biochar flocculation and leads to biochar-mineral complexes formation (Cheng et al., 2006; Lin et al., 2012; Jien and Wang, 2013; Fan et al., 2018). Six et al. (2004) stated that the addition of organic matter electrostatically joins the soil particles. Previous studies showed that SIFs may reach 100–1,000 atm and they determined soil aggregate swelling, dispersion, and breakdown in aqueous systems (Hu et al., 2015). Our results indicated that soil net internal force decreased with increasing biochar addition (Fig. 4). This calculation fits the experimental data (Fig. 5), demonstrating that biochar addition lowers net soil internal force and increases soil aggregate stability. Yu et al. (2017) performed an 8-month straw incubation study and found that an increase in SOM stabilizes soil aggregates by lowering the net pressure of SIFs. Annabi et al. (2007) reported that organic material stabilizes the aggregates by increasing interparticle aggregate cohesion, but they did not quantified the cohesion force. In addition, soil hydrophobicity also stabilizes aggregates and could reduce the slaking effect (Le Bissonnais, 1996; Derjaguin et al., 1987; Sullivan, 1990; Doerr and Thomas, 2000; Joseph et al., 2010). However, Dal Ferro et al. (2012) described the relatively little effect of hydrophobicity of organic content input for the stability of soil aggregate, especially for the case of large carbon input soils. Furthermore, previous studies showed that the air pressure produced by the slaking effect was <1 atm (Vachaud et al., 1973; Zaher et al., 2005), which is far lower than the SIFs (100–1000 atm). Therefore, the SIFs show to play a critical role in the stability of soil aggregates.

The relationship of soil aggregate stability with electrolyte concentration mirrors the relationship of SIFs from theoretic calculation by using soil surface properties with electrolyte concentration (Figs. 4 and 5), pointing to the fact that the net pressure of SIFs markedly affects aggregate stability in biochar-amended soils. The classic double layer theory states that the decrease in electrolyte concentration of bulk solution leads to an increase in the electric field of soil colloids. At the same time, the electrostatic repulsive forces increase and the soil aggregates disperse (Quirk, 1994; McBride, 1997; Hu et al., 2015; Yu et al., 2020). Laegdsmand et al. (1999) have shown that colloidal particles flocculate in response to increasing ionic strength. In contrast, colloid dispersion increases with decreasing ionic strength. Hence, as the rain enters the soil, the bulk solution electrolyte concentration is reduced by dilution, and the soil electrostatic repulsive force and soil aggregate breakdown increase.

5. Conclusions

In this study, we employed the simplified Na^+-saturated aggregates to quantitatively study the effects of biochar amendments on SIFs and aggregate stability. We found that SOM, CEC, SSA, σ_0 and aggregate stability increased with biochar addition rates after two years. However, the biochar amendment caused soil pH to decrease slightly. Calculations disclosed that repulsive and attractive forces of soil increased in response to biochar addition. The biochar amendment caused the net pressure of SIFs to decrease. These theoretical results agreed well with our experimental data for Na^+-saturated aggregate stability and thus soil aggregate stability. Overall, we conclude that biochar application improves soil surface properties, decreases the repulsive net pressure between soil particles, and finally stabilizes soil aggregates. However, the simplification in our experiments, including pretreatments, measurements under electrolyte solution, substantially differed from in situ conditions, which must be kept in mind. Nevertheless, even after simplification and laboratory control, the approach adopted here did generate important quantitative information. This initial result provides a stepping stone for evaluating the effect of biochar on aggregate stability by providing information about interaction forces between soil particles in a quantitative manner.

Declaration of Competing Interest

The authors declare that they have no known competing financial interests or personal relationships that could have appeared to influence the work reported in this paper.

Acknowledgments

This work was supported by the National Natural Science Foundation of China (41977024, 41701261 and 41601236), and the Natural Science Foundation of Shaanxi Province (2018JQ4005).

Appendix A. Supplementary data

Supplementary data to this article can be found online at https://doi.org/10.1016/j.geoderma.2021.115276.

References

Abrishamkesh, S., Gorji, M., Asadi, H., Bagheri-Marandi, G.H., Pourbabaee, A.A., 2015. Effects of rice husk biochar application on the properties of alkaline soil and lentil growth. Plant Soil Environ. 61, 475–482.
Ackler, H.D., French, R.H., Chiang, Y.M., 1996. Comparison of Hamaker constants for ceramic systems with intervening vacuum or water: From force laws and physical properties. J. Colloid Interface Sci. 179, 460–469.
Alwabel, M.I., Hussain, Q., Usman, A.R., Ahmad, M., Abduljabbar, A.S., Sallam, A.S., Ok, Y.S., 2018. Impact of biochar properties on soil conditions and agricultural sustainability: A review. Land Degrad. Dev. 29, 2124–2161.
Amézketa, E., 1999. Soil aggregate stability: a review. J. Sustain. Agr. 14, 83–151.
Annabi, M., Houot, S., Francou, C., Poitrenaud, M., Le Bissonnais, Y., 2007. Soil aggregate stability improvement with urban composts of different maturities. Soil Sci. Soc. Am. J. 71, 413–423.
Arif, M., Ilyas, M., Riaz, M., Ali, K., Shah, K., Ul Haq, I., Fahad, S., 2017. Biochar improves phosphorus use efficiency of organic-inorganic fertilizers, maize-wheat productivity and soil quality in a low fertility alkaline soil. Field Crop. Res. 214, 25–37.
Bergstrom, L., 1997. Hamaker constants of inorganic materials. Adv. Colloid Interface Sci. 125–169.
Bolan, N.S., Naidu, R., Syers, J.K., Tillman, R.W., 1999. Surface charge and solute interactions in soils. Adv. Agron. 67, 87–140.
Borchard, N., Siemens, J., Ladd, B., Möller, A., Amelung, W., 2014. Application of biochars to sandy and silty soil failed to increasemaize yield under common agricultural practice. Soil Tillage Res. 144, 184–194.
Bronick, C.J., Ral, R., 2005. Soil structure and management: a review. Geoderma 124, 3–22.
Burrell, L.D., Zehetner, F., Rampazzo, N., Wimmer, B., Soja, G., 2016. Long-term effects of biochar on soil physical properties. Geoderma 282, 96–102.
Chan, K.Y., Xu, Z., 2009. Biochar: nutrient properties and their enhancement. Biochar Environ. Manag. Sci. Technol. 1, 67–84.

Cheng, C.H., Lehmann, J., Engelhard, M.H., 2008. Natural oxidation of black carbon in soils: Changes in molecular form and surface charge along a climosequence. Geochim. Cosmochim. Ac. 72, 1598–1610.
Cheng, C.H., Lehmann, J., Thies, J.E. Burton, S.D., M.H., Engelhard, M.H., 2006. Oxidation of black carbon by biotic and abiotic processes. Org. Geochem. 37, 1477–1488.
Dal Ferro, N., Berti, A., Franciso, O., Ferrari, E., Matthews, G.P., Morari, F., 2012. Investigating the effects of wettability and pore size distribution on aggregate stability: The role of soil organic matter and the humic fraction. Eur. J. Soil Sci. 63, 152–164.
Derjaguin, B.V., Churaev, N.V., Muller, V.M., 1987. Surface Forces, Consult. Bur. New York. 440, 1–23.
Ding, W.Q., Liu, X.M., Hu, F.N., Zhu, H.L., Luo, Y.X., Li, S., Li, H., 2019. How the particle interaction forces determine soil water infiltration: Specific ion effects. J. Hydrol. 568, 492–500.
Doerr, W.A., Thomas, A.D., 2000. The role of soil moisture in controlling water repellency: New evidence from forest soils in Portugal. J. Hydrol. 231–232, 134–147.
El-Naggar, A., Lee, S.S., Rinklebe, J., Farooq, M., Song, H., Sarmah, A.K., Zimmerman, A. R., Ahmad, M., Shaheen, S.M., Ok, Y.S., 2019. Biochar application to low fertility soils: A review of current status, and future prospects. Geoderma 337, 536–554.
El-Naggar, A.H., Usman, A.R.A., Al-Omran, A., Ok, Y.S., Ahmad, M., Al-Wabel, M.I., 2015. Carbon mineralization and nutrient availability in calcareous sandy soils amended with woody waste biochar. Chemosphere 138, 67–73.
Fan, Q.Y., Sun, J.X., Chu, L., Cui, L.Q., Quan, G.X., Yan, J.L., Hussain, Q., Iqbal, M., 2018. Effects of chemical oxidation on surface oxygen-containing functional groups and adsorption behavior of biochar. Chemosphere 207, 33–40.
Farres, P.J., 1980. Some observations on the stability of soil aggregates to raindrop impact. Catena 7, 223–231.
Fungo, B., Lehmann, J., Kalbitz, K., Thiongo, M., Okeyo, I., Tenywa, M., Neufeldt, H., 2017. Aggregate size distribution in a biochar-amended tropical Ultisol under conventional hand-hoe tillage. Soil Tillage Res. 165, 190–197.
Gao, S., DeLuca, T.H., Cleveland, C.C., 2019. Biochar additions alter phosphorus and nitrogen availability in agricultural ecosystems: a meta-analysis. Sci. Total Environ. 654, 463–472.
Glaser, B., Balashov, E., Haumaier, L., Guggenberger, G., Zech, W., 2000. Black carbon in density fractions of anthropogenic soils of the Brazilian Amazon region. Org Geochem 31, 669–678.
Gong, Y., Tian, R., Li, H., 2018. Coupling effects of surface charges, adsorbed counterions and particle-size distribution on soil water infiltration and transport. Eur. J. Soil Sci. 69, 1008–1017.
Hartley, W., Riby, P., Waterson, J., 2016. Effects of three different biochars on aggregate stability, organic carbon mobility and micronutrient bioavailability. J. Environ. Manage. 181, 770–778.
Haynes, R.J., Naidu, R., 1998. Influence of lime, fertilizer and manure applications on soil organic matter content and soil physical conditions: a review. Nutrient Cycl. Agroecosyst. 51, 123–137.
Herath, H.M.S.K., Camps-Arbestain, M., Hedley, M., 2013. Effect of biochar on soil physical properties in two contrasting soils: an Alfisol and an Andisol. Geoderma 209, 188–197.
Hu, F.N., Liu, J.F., Xu, C.Y., Du, W., Yang, Z.H., Liu, X.M., Liu, G., Zhao, S.W., 2018a. Soil internal forces contribute more than raindrop impact force to rainfall splash erosion. Geoderma 330, 91–98.
Hu, F.N., Liu, J.F., Xu, C.Y., Wang, Z.L., Liu, G., Li, H., Zhao, S.W., 2018b. Soil internal forces initiate aggregate breakdown and splash erosion. Geoderma 320, 43–51.
Hu, F.N., Xu, C.Y., Li, H., Li, S., Yu, Z., Li, Y., He, X.H., 2015. Particles interaction forces and their effects on soil aggregates breakdown. Soil Tillage Res. 147, 1–9.
Huang, P.M., 2004. Soil mineral–organic matter–microorganism interactions: fundamentals and impacts. Adv. Agron. 82, 391–472.
Huang, X.R., Li, H., Li, S., Xiong, H.L., Jiang, X.J., 2016. Role of cationic polarization in humus-increased soil aggregate stability. Eur. J. Soil Sci. 67, 341–350.
Jien, S.H., Wang, C.S., 2013. Effects of biochar on soil properties and erosion potential in a highly weathered soil. Catena 110, 225–233.
Joseph, S.D., Camps-Arbestain, M., Lin, Y., Munroe, P., Chia, C.H., Hook, J., Zwieten, L., Kimber, S., Cowie, A., Singh, B.P., Lehmann, J., Foidl, N., Smernik, R.J., Amonette, J. E., 2010. An investigation into the reactions of biochar in soil. Soil Res. 48, 501–515.
Jenkinson, S.J., Kalembasa, D.S.A., 1973. Comparative study of titrimetric and gravimetric methods for the determination of organic carbon in soil. J. Sci. Food. Agr. 24, 1085–1090.
Laegdsmand, M., Villholth, K.G., Ullum, M., Jensen, K.H., 1999. Processes of colloid mobilization and transport in macroporous soil monoliths. Geoderma 93, 33–59.
Laghari, M., Mirjat, M.S., Hu, Z.Q., Fazal, S., Xiao, B., Hu, M., Chen, Z.H., Guo, D.B., 2015. Effects of biochar application rate on sandy desert soil properties and sorghum growth. Catena 135, 313–320.
Laird, D.A., Fleming, P., Davis, D.D., Horton, R., Wang, B.Q., Karlen, D.L., 2010. Impact of biochar amendments on the quality of a typical midwestern agricultural soil. Geoderma 158, 443–449.
Le Bissonnais, Y., 1996. Aggregate stability and assessment of soil crustability and erodibility: I. Theory and methodology. Eur. J. Soil Sci. 47, 425–437.
Lehmann, J., 2007. Bio-energy in the black. Front. Ecol. Environ. 5, 381–387.
Lentz, R.D., Ippolito, J.A., 2012. Biochar and manure affect calcareous soil and corn silage nutrient concentrations and uptake. J. Environ. Qual. 41, 1033–1043.
Li, H., Hou, J., Liu, X.M., Li, R., Zhu, H., Wu, L.S., 2011. Combined determination of specific surface area and surface charge properties of charged particles from a single experiment. Soil Sci. Soc. Am. J. 75, 2128–2135.
Li, H., Qing, C., Wei, S.Q., Jiang, X.J., 2004. An approach to the method for determination of surface potential on solid/liquid interface: theory. J. Colloid Interface Sci. 275, 172–176.
Li, S., Li, H., Hu, F.N., Huang, X.Y., Xie, D.T., Ni, G.P., 2015. Effects of strong ionic polarization in the soil electric field on soil particle transport during rainfall. Eur. J. Soil Sci. 66, 921–929.
Li, S., Li, H., Xu, C.Y., Huang, X.R., Xie, D.T., Ni, J.P., 2013. Particle interaction forces induce soil particle transport during rainfall. Soil Sci. Soc. Am. J. 77, 1563–1571.
Li, S.Z., Xu, R.K., 2008. Electrical double layers' interaction between oppositely charged particles as related to surface charge density and ionic strength. Colloid Surf. A. 326, 157–161.
Li, Y.Y., Zhang, F.B., Yang, M.Y., Zhang, J., Xie, Y.Q., Xie, Y.G., 2019. Impacts of biochar application rates and particle sizes on runoff and soil loss in small cultivated loess plots under simulated rainfall. Sci. Total Environ. 649, 1403–1413.
Liang, B., Lehmann, J., Solomon, D., Kinyangi, J., Grossman, J., O'Neill, J.B., Skjemstad, J.O., Thies, J., Luizao, F.J., Petersen, J., Neves, E.G., 2006. Black Carbon Increases Cation Exchange Capacity in Soils. Hortic. Sci. 70, 1719–1730.
Liang, Y., Hilal, N., Langston, P., Starov, V., 2007. Interaction forces between colloidal particles in liquid: theory and experiment. Adv. Colloid Interf. Sci. 134, 151–166.
Lin, Y., Munroe, P., Joseph, S., Kimber, S., Van Zwieten, L., 2012. Nanoscale organo-mineral reactions of biochars in ferrosol: an investigation using microscopy. Plant Soil 357, 369–380.
Liu, Z.X., Chen, X.M., Jing, Y., Li, Q.X., Zhang, J.B., Huang, Q.R., 2014. Effects of biochar amendment on rapeseed and sweet potato yields and water stable aggregate in upland red soil. Catena 123, 45–51.
Liu, J.F., Wang, Z.L., Hu, F.N., Xu, C.Y., Ma, R.T., Zhao, S.W., 2020. Soil organic matter and silt contents determine soil particle surface electrochemical properties across a long-term natural restoration grassland. Catena 190, 104526.
Liu, X.H., Zhang, X.C., 2012. Effect of biochar on pH of alkaline soils in the loess plateau: results from incubation experiments. Int. J. Agric. Biol. 14, 745–750.
Lu, S.G., Sun, F.F., Zong, Y.T., 2014. Effect of rice husk biochar and coal fly ash on some physical properties of expansive clayey soil (Vertisol). Catena 114, 37–44.
Luo, C.Y., Yang, J.J., Chen, W., Han, F.P., 2020. Effect of biochar on soil properties on the Loess Plateau: Results from field experiments. Geoderma 369, 114323.
Lychuk, T.E., Izaurralde, R.C., Hill, R.L., McGill, W.B., Williams, J.R., 2014. Biochar as a global change adaption: predicting biochar impacts on crop productivity and soil quality for a tropical soil with Environmental Policy Integrated Climate (EPIC) model. Mitig. Adapt. Strateg. Glob. Change. 142, 160–167.
Mukherjee, A., Lal, R., 2013. Biochar impacts on soil physical properties and greenhouse gas emissions. Agronomy. 3, 313–339.
Mukherjee, A., Zimmerman, A.R., Harris, W.G., 2011. Surface chemistry variations among a series of laboratory-produced biochars. Geoderma 163, 247–255.
McBride, M.B., 1997. A critique of diffuse double layer models applied to colloid and surface chemistry. Clay Clay Miner. 45, 598–608.
Ojeda, G., Mattana, S., Avila, A., Alcaniz, J.M., Volkmann, M., Bachmann, J., 2015. Are soil-water functions affected by biochar application? Geoderma 249, 1–11.
Omondi, M.O., Xia, X., Nahayo, A., Liu, X., Korai, P.K., Pan, G., 2016. Quantification of biochar effects on soil hydrological properties using meta-analysis of literature data. Geoderma 274, 28–34.
Palansooriya, K.N., Ok, Y.S., Awad, Y.M., Lee, S.S., Sung, J.K., Koutsospyros, A., Moon, D.H., 2019. Impacts of biochar application on upland agriculture: A review. J. Environ. Manage. 234, 52–64.
Peng, X., Ye, L.L., Wang, C.H., Zhou, H., Sun, B., 2011. Temperature- and durationdependent rice straw-derived biochar: characteristics and its effects on soil properties of an Ultisol in southern China. Soil Tillage Res. 112, 159–166.
Purakayastha, T.J., Kumari, S., Pathak, H., 2015. Characterisation, stability, and microbial effects of four biochars produced from crop residues. Geoderma 239, 293–303.
Qian, L.B., Chen, B.L., 2014. Interactions of aluminum with biochars and oxidized biochars: implications for the biochar aging process. J. Agric. Food Technol. 62, 373–380.
Quirk, J.P., 1994. Internal forces: a basis for the interpretation of soil physical behavior. Adv. Agron. 53, 122–184.
Rabot, E., Wiesmeier, M., Schlüter, S., Vogel, H.J., 2018. Soil structure as an indicator of soil functions: a review. Geoderma 314, 122–137.
Rengasamy, P., Tavakkoli, E., McDonald, G.K., 2016. Exchangeable cations and clay dispersion: Net dispersive charge, a new concept for dispersive soil. Eur. J. Soil Sci. 7, 659–665.
Resurreccion, A.C., Moldrup, P., Tuller, M., Ferré, T.P.A., Kawamoto, K., Komatsu, T., de Jonge, L.W., 2011. Relationship between specific surface area and the dry end of the water retention curve for soils with varying clay and organic carbon contents Water Resour. Res. 47, 240–250.
Six, J., Bossuyt, H., Degryze, S., Denef, K., 2004. A history of research on the link between (micro)aggregates, soil biota, and soil organic matter dynamics. Soil Tillage Res. 79, 7–31.
Six, J., Elliott, E.T., Paustian, K., 2000. Soil macroaggregate turnover and microaggregate formation: a mechanism for C sequestration under no-tillage agriculture. Soil Biol. Biochem. 32, 2099–2103.
Sohi, S.P., Krull, E., Lopez-Capel, E., Bol, R., 2010. A review of biochar and its use and function in soil. Adv. Agron. 105, 47–82.
Soinne, H., Hovi, J., Tammeorg, P., Turtola, E., 2014. Effect of biochar on phosphorus sorption and clay soil aggregate stability. Geoderma 219, 162–167.
Spokas, K.A., Koskinen, W.C., Baker, J.M., Reicosky, D.C., 2009. Impacts of woodchip biochar additions on greenhouse gas production and sorption/degradation of two herbicides in a Minnesota soil. Chemosphere 77, 574–581.

Suddick, E.C., Six, J., 2013. An estimation of annual nitrous oxide emissions and soil quality following the amendment of high temperature walnut shell biochar and compost to a small scale vegetable crop rotation. Sci. Total Environ. 465, 298–307.
Sullivan, L.A., 1990. Soil organic matter, air encapsulation and water-stable aggregation. J. Soil Sci. 41, 529–534.
Tisdall, J.M., Oadcs, J.M., 1982. Organic matter and water-stable aggregates in soils. J. Soil Sci. 33, 141–163.
Tuller, M., Or, D., 2005. Water films and scaling of soil characteristic curves at low water contents. Water Resour. Res. 41, 315–335.
Vachaud, G., Vauclin, M., Khanji, D., Wakil, M., 1973. Effects of air pressure on water flow in an unsaturated stratified vertical column of sand. Water Resources Res. 9, 160–173.
Van Oost, K., Quine, T.A., Govers, G., Gryze, D., Six, J., Harden, J.W., Ritchie, J.C., McCarty, G.W., Heckrath, G., Kosmas, C., Giraldez, J.V., Marques da Silva, J.R., Merckx, R., 2007. The impact of agricultural soil erosion on the global carbon cycle. Science 318, 626–629.
Wang, C.L., Xu, C.Y., Zhao, S.W., Hu, F.N., Li, Q.R., 2020. Effect of organic matter removal on stability of suspension of loess nanoparticles. Acta Pedologica Sinica 57, 119–129.
Wang, D., Fonte, S.J., Parikh, S.J., Six, J., Scow, K.M., 2017. Biochar additions can enhance soil structure and the physical stabilization of C in aggregates. Geoderma 303, 110–117.
Wang, J.Y., Xiong, Z.Q., Kuzyakov, Y., 2016. Biochar stability in soil: meta-analysis of decomposition and priming effects. Gcb Bioenergy 8, 512–523.
Watanabe, K., Mizoguchi, M., 2002. Amount of unfrozen water in frozen porous media saturated with solution. Cold Reg. Sci. Tech. 34, 103–110.
Xu, C.Y., Li, H., Hu, F.N., Li, S., Liu, X.M., Li, Y.T., 2015. Non-classical polarization of cations increases the stability of clay aggregates: specific ion effects on the stability of aggregates. European J. Soil Sci. 66, 615–623.
Xu, C.Y., Zhou, T.T., Wang, C.L., Liu, H.Y., Zhang, C.T., Hu, F.N., Zhao, S.W., Geng, Z.C., 2020. Aggregation of polydisperse soil colloidal particles: Dependence of Hamaker constant on particle size. Geoderma. 359, 113999.
Xu, R.K., Zhao, A.Z., Yuan, J.H., Jiang, J., 2012. pH buffering capacity of acid soils from tropical and subtropical regions of China as influenced by incorporation of crop straw biochars. J. Soil Sediment. 12, 494–502.
Yu, Z.H., Zheng, Y.Y., Zhang, J.B., Zhang, C.Z., Ma, D.H., Chen, L., Cai, T.Y., 2020. Importance of soil internal forces and organic matter for aggregate stability in a temperate soil and a subtropical soil. Geoderma 362, 114088.
Yu, Z.H., Zhang, J.B., Zhang, C.Z., Xin, X.L., Li, H., 2017. The coupling effects of soil organic matter and particle interaction forces on soil aggregate stability. Soil Tillage Res. 174, 251–260.
Yuan, J., Xu, R., 2011. The amelioration effects of low temperature biochar generated from nine crop residues on an acidic ultisol. Soil Use Manage. 27, 110–115.
Zaher, H., Caron, J., Ouaki, B., 2005. Modeling aggregate internal pressure evolution following immersion to quantify mechanisms of structural stability. Soil Sci. Soc. Am. J. 69, 1–12.
Zhang, F.B., Huang, C.H., Yang, M.Y., Zhang, J.Q., Shi, W.Y., 2019. Rainfall simulation experiments indicate that biochar addition enhances erosion of loess-derived soils. Land Degrad. Dev. 30, 2272–2286.
Zhang, Q.Z., Du, Z.L., Lou, Y.L., He, X.H., 2015. A one-year short-term biochar application improved carbon accumulation in large macroaggregate fractions. Catena 127, 26–31.
Zhang, Q.Q., Song, Y.F., Wu, Z., Yan, X.Y., Gunina, A., Kuzyakov, Y., Xiong, Z.Q., 2020a. Effects of six-year biochar amendment on soil aggregation, crop growth, and nitrogen and phosphorus use efficiencies in a rice-wheat rotation. J. Clean. Prod. 242, 118435.
Zhang, X., Qu, J., Li, H., La, S., Tian, Y.Q., Gao, L.H., 2020b. Biochar addition combined with daily fertigation improves overall soil quality and enhances water-fertilizer productivity of cucumber in alkaline soils of a semi-arid region. Geoderma 363, 114170.
Zhao, L., Cao, X.D., Zheng, W., Wang, Q., Yang, F., 2015. Endogenous minerals have influences on surface electrochemistry and ion exchange properties of biochar. Chemosphere 136, 133–139.
Zhao, Z.Z., Zhou, W.J., 2019. Insight into interaction between biochar and soil minerals in changing biochar properties and adsorption capacities for sulfamethoxazole. Environ. Pollut. 25, 208–217.